RESEARCH ARTICLE

Description of the Hydrogeochemical Mechanisms in Shallow Groundwater Using a Combined Approach of Geochemical and Geostatistical Methods in Idu Abuja

Iyi, Emmanuel Chibuike

Department of Geology and Mining, Enugu State University of Science and Technology, Enugu, Nigeria

Corresponding Authors: *Iyi Emmanuel Chibuike, Department of Geology and Mining, Enugu State University of Science and Technology, Enugu, Nigeria*

ABSTRACT

Hydrogeochemical studies were performed in the Idu and adjacent areas of Nigeria's federal capital territory, Abuja. 25 groundwater samples were gathered from 15 existing boreholes and 10 shallow hand dug wells. Based on the synthesis of standard geochemical approaches plus GIS and geostatistical tools, geochemical processes and conditions regulating groundwater chemistry are described. The analyses of the ionic ratios and Gibbs charts indicate that the processes of rock/water contacts, accompanied by ion exchange, and decomposition of carbonate and silicate rocks affected the groundwater composition of the research area. A transition from less mineralized Mg^{2+}-CO_3^{2-}-Cl^-, Mg^{2+}-Ca^{2+}-Cl^- and Mg^{2+}-Ca^{2+}-CO_3^{2-} type of water to elevated mineralized Mg^{2+}-Cl^- water types is demonstrated by the hydrogeochemical properties of groundwater. Utilizing cluster analysis, three groups have been identified, namely C1 and C2. The Na^+/Cl^-, Mg^{2+}/Ca^{2+} and Cl^-/HCO_3^- ratios and EC contents of the spatial distribution maps suggest that carbonate and silicate rocks weathering played a big role on the eastern halves of the research districts in groundwater chemistry. However, due to the effect of the convection-precipitation process as well as water/rock contacts on the western portions of the study region, the acidification process has risen.

Keywords: *Hydrogeochemical; Mechanism; GIS; Geostatistical and Geochemical Methods; Ionic ratio; Basement Complex; Shallow Groundwater*

Introduction

In a tropical climate, groundwater plays a prominent part in water supply and ecosystem (Isa et al., 2012). Groundwater quality is critical in order to sustain life (Appelo and Postma, 1994). Anthropogenic and geogenic influences like geological features, rainfall concentration, geochemical processes, the interplay between aquifers and groundwater nutrients, as well as human activities governs groundwater quality (Ifediegwu et al., 2019). Different water types result from the interplay of these relevant factors (Jalali, 2005b). The composition of groundwater relies on various hydrogeochemical mechanisms that the groundwater experiences over a period of time.

In tropical regions, like Idu in Abuja, the federal capital territory of Nigeria, so many processes evapotranspiration, salty water, ion exchange, separation and dissolution of minerals, oxidation reduction as well as biological factors maybe active in chemical makeup of groundwater at the same time. Acidification is among the key problems of the water crisis that has become a significant hazard to the freshwater quality that is sufficient for human consumption. The activities of land use, changes in climate and the geological environment own a massive impact on the salty content of groundwater (Salama et al., 1999). Inappropriate dumping of solid wastes and drainage techniques in tropical regions also could raise the risk of gradual soil salinization due to the accumulation of solvents in irrigation water (Isa et al., 2012). So many researches have demonstrated the function of various mechanisms like elevated rate of evaporation and constrained discharge, too much pumping of groundwater, fossil saltwater, and saltwater-freshwater mixing that improves the dissolved salts in the groundwater (Ifediegwu, 2019;

Demirel and Turkmen, 2001). The region of Idu on the northern edge of Abuja is under growing human pressure due to rising population and industrial production. Groundwater supplies along the coastline could endanger via the mixing process of saltwater intruding into the freshwater, owing to the excess exploitation of groundwater (Ohwoghere-Asuma and Essi, 2017; Aris et al., 2010).

Since acidification on the Idu in Abuja could be as a result of mixture of multiple mechanisms; present study was designed to examine the origin of groundwater quality as well as to ascertain the hydrogeochemical mechanisms associated with the acidification of groundwater in the research area.

In the southern section of the research region, where plain is bordered by the granitic hills, the climate conditions, elevation, and geological structure are distinct. The hydrochemistry of the groundwater within the hills could be affected via the dissolving of crystalline rocks, ion exchange and the oxidation of dissolved ions as the predominant mechanisms. Hanshaw and Back (1979) mentioned that, due to the quick dissolution/rainfall catalysis of carbonate rocks, crystalline aquifers form a complex geochemical process with water-rock interaction.

Examination of the key ions was utilized to define the hydrogeochemical facies of the water. Many scholars have investigated the groundwater chemistry and identified hydrogeochemical mechanisms by creating geochemical models and visual tools for the interpretations of water quality indicators (Ravikumar et al., 2013; Retnam et al., 2013; Ifediegwu et al., 2019; Sisodia and Moundiotiva, 2006; Reddy and Kumar, 2010). Multivariate statistical methods combined with PHREEQC software and GIS tools have been used in recent decades to determine potential hydrogeochemical data information in dynamic processes (Hamzah et al., 2017). This systematic approach would be helpful to determine and map various physico-chemical parameters in diverse groundwater aquifers. The integration of hydrogeochemical devices and statistical investigation has been used to examine the groundwater characteristics between the sampling locations. The use of GIS offers a coherent method of representing the physico-chemical characteristics of groundwater in a particular region, and also displaying the distribution pattern of the hydrogeochemical parameters of groundwater in thematic maps (Hamzah et al., 2017). The GIS approach based on the ionic ratios of Na^+/Cl^-, Mg^{2+}/Ca^{2+} and Cl^-/HCO_3^- and EC are indeed an effort to explain the fluctuations in the characteristics of groundwater through the spatial dispensation maps (Narany et al., 2014). Although GIS is an ideal approach for mapping, querying and analysing data that may be beneficial for the management to control the natural resource in a specific region, few investigations have been performed with present approach in groundwater hydrochemical assessment.

Sustainable water resource production in tropical regions is highly dependent on the evaluation of groundwater hydrogeochemical evolution. However, there is minimal research on the hydro-chemical properties of the Idu and environs in Abuja. This research seeks to explore the key hydrogeochemical features of Idu and Environ's groundwater quality, and also offering a description of the distribution pattern of ionic groundwater ratios through GIS and interpolation strategies.

Materials and Methods
Location, physiography and climate of the study area
Idu is an industrial layout found in the northeastern part of Abuja, the capital territory of Nigeria and is positioned between 7°20'E and 7°30'E longitudes and 9°03'N and 9°13'N latitudes (Fig. 1). The area encompasses 7,770 km^2 of surface area. Idu and environs are shares boundary with Budupe in the north, in the east by Karu, in the south by Lugbe and in the west by Gwagwa each.

Topographically, the study region is visualized into three vast landforms; the hilly clusters of the northern section; the gently rolling plains occupying the central regions and the craggy nature of rugged and shapeless granitic hills characterized majorly by broken rock boulders surrounding the southern segment of the research district. Generally, the elevation of the area ranged from 91m in the south to over 960m to the north. Gurara, Usman, and Tapa are the biggest rivers in the research district. These rivers originate from the granitic hills and flow into the River Niger. The Gurara River flows on the eastern section of the Gudu and move via the Kaura area. These rivers are primary means of agricultural activity in the district. The Gurara River extends up to 185 km with mean yearly discharge of 723mcm. The Usman River transverses via Wuse 1. The mean yearly flow is 341mcm. The Tapa River on the northern edge of the research district flows to roughly 60 km from Idu to its confluence with Usman River. The mean yearly discharge rate is about 265mcm. Rainfall in the area occur during the wet season which span from April to November with average of 1520mm per annum. Approximately 29.5°C is the main annual temperature. From the north of the area to the south, the temperature decreases. The regular evaporation is around 643 mm.

IYI

Geology and Hydrogeology

The prevalent and most extended rock in the central and western segments of the research district is the migmatite-gneiss complex which the age varied from Neo- Proterozoic to Meso-Archean (542Ma-3200Ma) and is made up of migmatites and banded gneisses whereas, the eastern segment of the study area is underlain by meta-sedimentary/volcanic series of Pre-Cambrian to Cambrian (800 ± 1100Ma) in age and composed of fine-grained flaggy quartzite and quartz schist. Occupying the northern area of the research district is the Pan-African Older Granitoids of Pan-African Orogeny (600 ± 200Ma) which consist mainly of porphyritic granite/coarse porphyritic biotite and biotite hornblende granite (Fig. 1).

Groundwater status of the research district is characterized by an unconfined and semi-confined aquifer.

The unconfined aquifer surrounds roughly 78% of the whole district while about 22% are limited to the area surrounded by semi-confined aquifer. Little quantity of water can be acquired in the freshly unweathered bedrock underneath the weathered strata. Groundwater is established majorly in the variable weathered/or transition zone and in fractures, joints and cracks of the basements. Fissure structures in the Basement Complex of Nigeria rarely extended up to 50m. The thickness of the aquifer ranges from lower than 10m for the migmatite-gneiss complex and Pan-African Older Granitoids to approximately 80m for the meta-sedimentary/volcanic series in the eastern regions of the research district. The movement of groundwater in fractured bedrock aquifers such as the research district is governed by topography and geological structures. In the research area groundwater flows from the recharge region (Maitama, Garki 2 and Gudu) in the northeastern parts to the discharge region (Furah and Tungan Daudu) in the southwestern segments of the research area. The hydraulic gradient fluctuates between 6 per thousand in the northeastern segment to 0.2 per thousand in the southwestern segment of the research district.
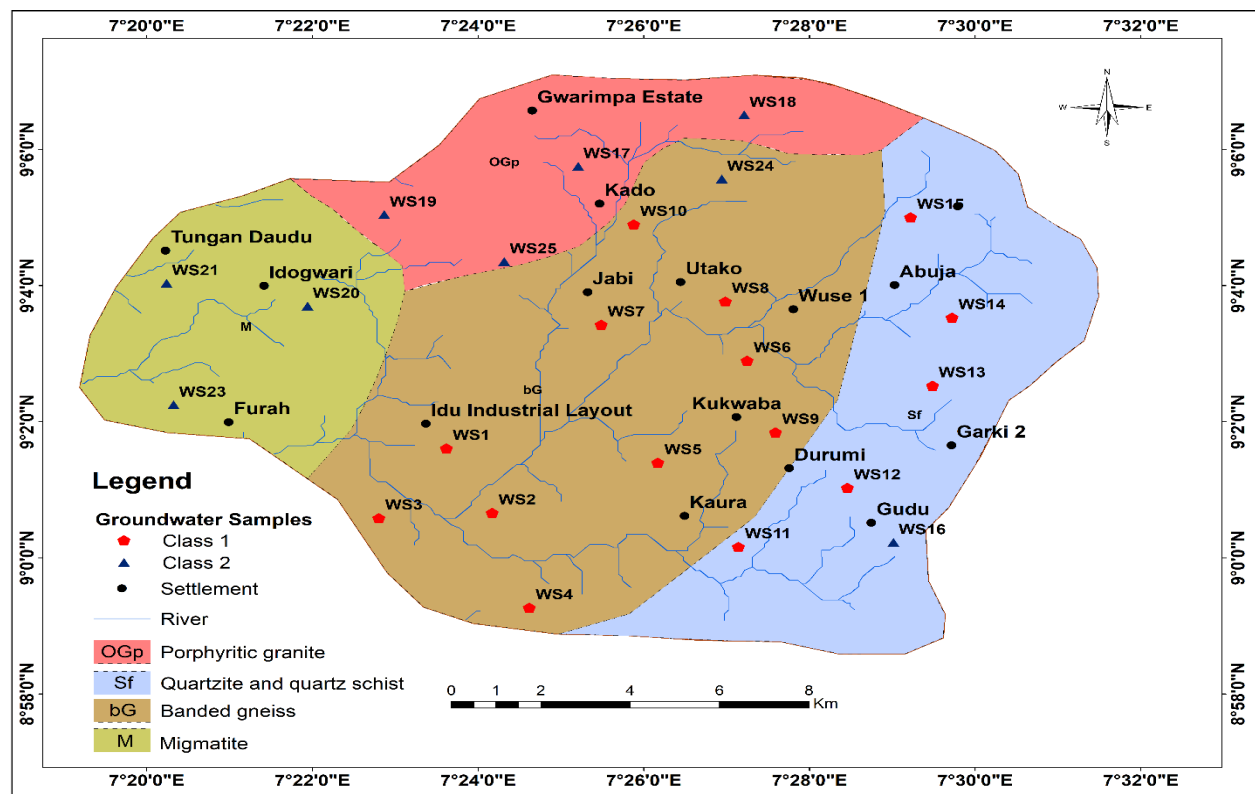

Fig. 1 Geologic Map of Idu and Environs

Groundwater Sampling and Analysis

Twenty-five groundwater samples were gathered from 15 existing boreholes and 10 shallow hand dug wells with 1litre acid-washed plastic containers. The containers were scrubbed several times with the groundwater to be analyzed prior to collection. The gathered samples were preserved at 4°C and conveyed to the laboratory within 24 hours of the sampling exercise. Instantly after sampling, physical parameters like temperature, pH, EC and TDS were directly examined in-situ with a multi-parameter portable meter (WP600 series meter). The gathered samples were examined for Ca^{2+}, Mg^{2+}, Na^+, K^+, Cl^-, SO_4^{2-}, HCO_3^- and CO_3^{2-} according to the APHA (2005) laboratory protocols. The Ca^{2+} and Mg^{2+} were measured titrimetrically adopting the approach of normal EDTA technique while Na^+ and K^+

were tested with flame photometry. CO_3^{2-} and HCO_3^- were analyzed adopting acid titration procedure, Cl by $AgNO_3$ titration procedure, sulphate and phosphate with spectrophotometer.

Statistical Analysis

Multivariate statistical evaluation was adopted to extract substantial data since hydro-chemical data sources in complicated process. To view the groundwater facies of the Idu-Karmo, chemical parameters were visually displayed employing Piper, Durov, Schoeller, and Gibbs diagrams. An approach of multivariate statistical analysis of correlation matrix, eigenvalues analysis (EA), and cluster analysis (CA) were carried out as quantitative and independent categorization algorithms of groundwater samples and to differentiate between the physicochemical properties and groundwater samples. Multivariate statistical examination uses naturally data sets (Triki et al., 2013). There is a significant skewing of the data for many other chemical parameters. The data ranged from 0 to +2. A normal distribution was only shown by values within the scale of -2 to +2, Na^+, K^+, NO_3^-, CO_3^{2-}, and pH weren't observed to be evenly distributed (Table 2). The data was then log-transformed so all the variables were normalized by calculating the total value and dividing by the standard deviation of variables prior to the multivariate examination. Separate examination was used to define and classify the characteristics of water into single and comprehensive categories according to the relationship between the variables. The classes will be discriminated by linear combinations of independent variables to reduce the error of miscategorization. DA was used to the original data adopting forward-step techniques to identify the most relevant variables that had a major impact on groundwater quality. The hierarchical dataset was used by the Ward approach to identify variables according to the similarities within a group and differences between the group cluster analyses. Agglomerative hierarchical cluster analysis (AHCA) was often used, beginning from the most related pair of items and formulating stronger clusters, where clusters were developed consecutively. A graphical description of the clustering process is given by the dendrogram, which presents an image of categories and their relative proximity. The level of linear relationship between two variables was summed up in this study utilizing Pearson's correlation matrix. Correlation values ranged from +1 to -1. Where +1 shows a highly significant correlation, -1 is a highly negative correlation, and 0 does not signify a linear correlation

Classification of Acidification Regions

An embedded platform to scrutinize the spatial dispensation of various ionic ratios like EC, Na^+/Cl^-, Mg^{2+}/Ca^{2+}, and Cl^-/HCO_3^- provided by the GIS and Geostatistical tools. The spatial dispensation maps of individual ratio, EC map was prepared employing the kriging model, which is among the perfect interpolation techniques in ArcGIS geostatistical extension (Nas and Berktay, 2010). Kriging is a technique for linear best possible effective interpolation with a lowest possible error function of the unsampled site, organized as follows

$$Z^* (x_o) = \sum_{i=1}^{n} n\lambda_i \, Z(x_i) \qquad (1)$$

Where $Z^* (x_o)$ represents the predicted value at site x_o, n represents the number of sites, $Z(xi)$ represents the known value at site xi, and λi represents the kriging weight. The simple geostatistical device for mapping the spatial autocorrelation of a heterogeneous data set is the semivariogram, which calculates the total level of distinction between the unsampled values and the closest data points (Journel and Keith, 1988). The investigational variogram's value for a gap distance of h is half the mean squared contrast among the value at $Z(xi)$ and $Z(xi+h)$ (Journel and Keith, 1988);

$$\Upsilon(h) = \frac{1}{2n \, (h)} \sum_{i=1}^{n(h)} [Z(x_i) - Z(x_i + h)^2 \qquad - \qquad - \qquad (2)$$

where $n(h)$ represents the number of data pairs between a specific category of distance and direction. The best suitable variogram model was selected by evaluating the experimental semivariogram and matching equivalent semivariogram, via classification algorithm. To give precise estimation in semivariograms, the nugget/sill ratio and the root-mean square error (RMSS) was implemented.

The ionic ratios like Ca^{2+}/Mg^{2+}, N^+/Cl^-, Cl^-/HCO_3^- and EC were considered as the most appropriate parameters for the exponential model (Table 1). The nugget/sill ratio ranged from 25 to 46% and the RMSS values ranged from 0.818 to 1.090, suggesting that there is a fairly minor bias and a high accuracy uncertainty value.

IYI

Table 1: Variographic Variables of the Groundwater Chemical Constituent in Idu and Environs

Ratio	Model	Nugget ($C0$)	Sill ($C_0 + C$)	(C_0/C_0+C) $*100$ Ratio	RMSS
Ca/Mg	Exponential	0.051	0.2018	25.27	0.818
Na/Cl	Exponential	0.098	0.2133	45.94	1.001
Cl/HCO3	Exponential	0.401	0.8942	44.84	1.082
EC (μS/cm)	Exponential	0.062	0.2116	29.30	1.090

Results and Discussion

In the cluster evaluation, groundwater samples were categorized in two broad groups comprising boreholes (class 1) and shallow hand dug wells (class 2), using a cluster analysis depending on the differences between the physicochemical properties of groundwater quality with respect to regular water (Fig. 2). The critical value of the physicochemical properties of Ca^{2+}, Mg^{2+}, Na^+, Cl^- and EC was calculated on the basis of the spatial variance of the groundwater sampling in the research district by discriminant analysis.

The samples had a related anionic structure in class 1 (boreholes) and class 2 (shallow hand dug wells) which was occupied by Cl^- with sequence orders of $Cl^- > HCO_3^- > SO_4^{2-}$ (meq/L) (Fig. 3). The samples in class 1 and class 2 (boreholes and shallow hand dug wells) had a cationic structure that was regulated by Mg^{2+} and Ca^{2+}, accordingly, with sequence arrangements of $Mg^{2+} \cong Ca^{2+} > Na^+$ (meq/L). Thus, the physicochemical properties of these categories were defined by the Mg-Ca-Cl water type. The samples in class 1 (boreholes) reflected the freshwater type owing to the average contents of TDS of about 691.68mg/L and EC around 1089.33 μS/cm, while the class 2 (shallow hand dug wells) water samples appeared to be brackish water with an average TDS content of 1029.3 mg/L and average EC content of 1104.5 μS/cm.

Table 2: Statistical Presentation of 25 Groundwater Samples Gathered from the Research Area

Parameters	Groundwater (Class 1)					Hand dug well (Class 2)				
	Min.	Max.	Mean	SD	Skewness	Min.	Max.	Mean	SD	Skewness
Temp.	20.1	25.8	23.9	1.72	-1.22	20	26.7	24.74	1.66	-2.15
pH	6.0	7.0	6.3	0.39	1.08	5.5	6.7	6.2	0.38	-0.09
EC	155	2230	1089.3	637.2	0.15	526	2210	1104.5	515.9	1.02
TSD	348.1	1092.6	691.7	243.5	-0.03	356	1002	644.3	225.5	0.19
$CaCO_3$	0.8	196	26.2	50.4	2.65	2.3	20.7	11.95	6.74	-0.14
Ca^{2+}	2.4	48.1	22.5	12.3	0.32	8.3	40	20.03	11.42	0.59
Mg^{2+}	19.5	145.9	72.3	33.4	0.43	35	117.4	76.49	23.51	-0.11
Na^+	2.9	50.0	22.4	15.4	0.40	6.3	33.3	18.03	7.76	0.46
K^+	3.3	23.7	7.0	4.7	2.83	4.1	23.7	15.11	6.15	-0.43
Fe^{3+}	0.02	0.4	0.09	0.12	1.98	0.02	0.13	0.06	0.03	0.88
Cl^-	35.5	215.8	113.3	64.4	0.47	42.5	209	99.81	53.09	0.83
NO_3^-	1.7	117.1	28.7	35.5	1.23	6.9	83	20.51	21.39	2.41
SO_4^{2-}	0.86	4.3	2.6	1.72	0.18	0.14	3.7	1.36	1.25	1.05
HCO_3^-	6	80	38	21.7	0.55	22	73	47.3	17.91	0.03
CO_3^{2-}	19	108	73.1	27.47	-0.08	33	99	58.7	18.75	0.58

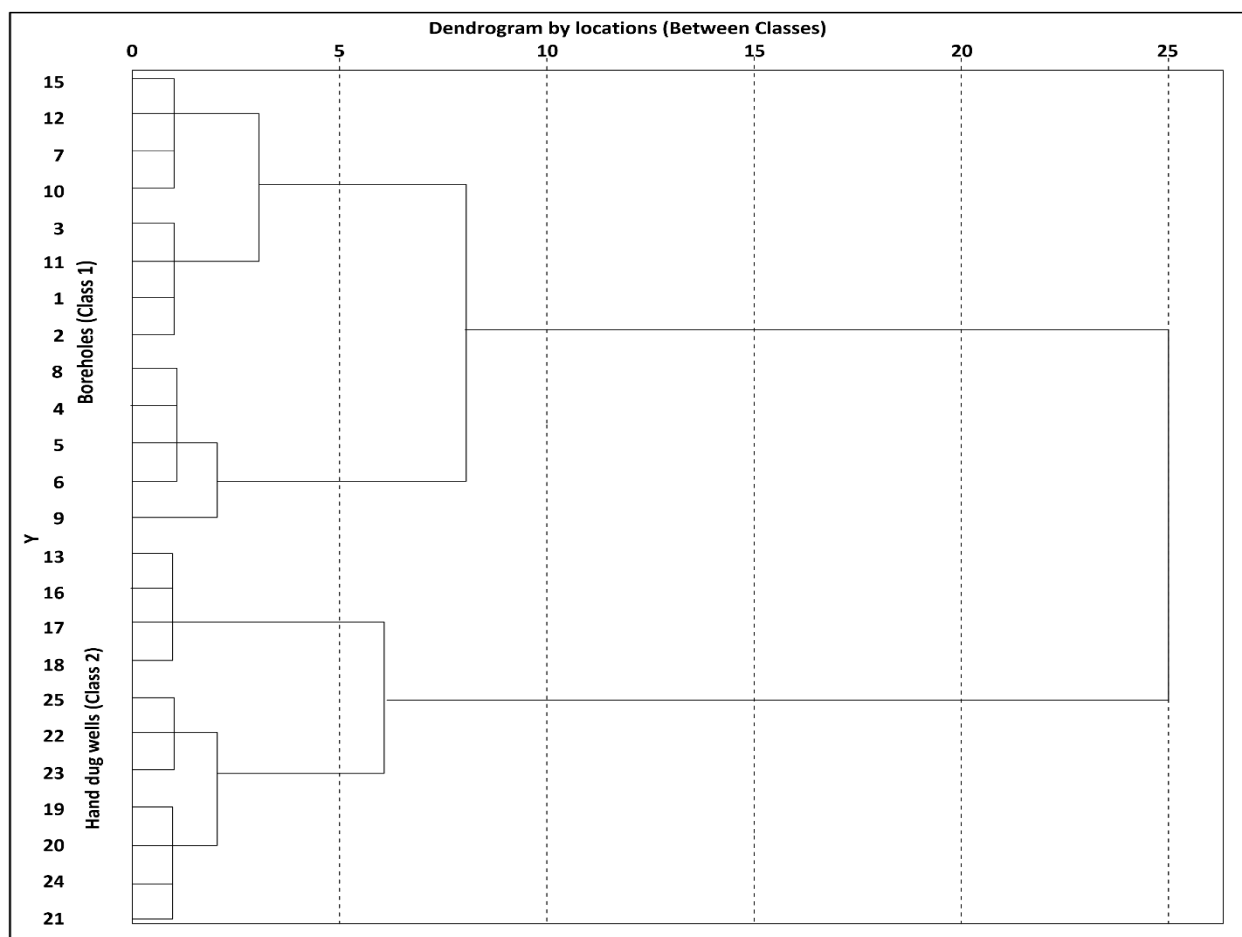**Fig. 2** Cluster Evaluation Diagram of the Research Area

Hydrogeochemical Facies.

In most sections of the study region, the Schoeller diagram revealed that Mg^{2+} and Cl^- are the prevalent ions (Fig. 3). Mg-Cl, mixed Mg-CO_3-Cl, Mg-Ca-Cl, Mg-Na-Cl and Mg-Ca-CO_3 types were seen in the bulk of groundwater samples. Owing to the crystalline phase transformation and large contact with granite, approximately 75 % of the groundwater were categorized as Mg-Cl type. Because it travelled from the east and western sections towards the central and southern sections of the research district, the groundwater type transformed into Mg-Ca-CO_3 and Mg-Ca-Cl (Fig. 4, 5, 6). The Mg-Ca-CO_3 water, which expanded to the Kaura, Durumi and Kukwaba, reflected irreversible groundwater hardness. Towards the northern and western sections of the area, the groundwater type modified to Mg-Na-Cl, which suggested the mildly salty water. The prevalent cation was found in the entire area of the study is Mg^{2+}, while Cl^- was the prominent anion. The spatial distribution map displayed that on the southcentral and western parts of the research district, the type of groundwater progressively varying from freshwater to salty water
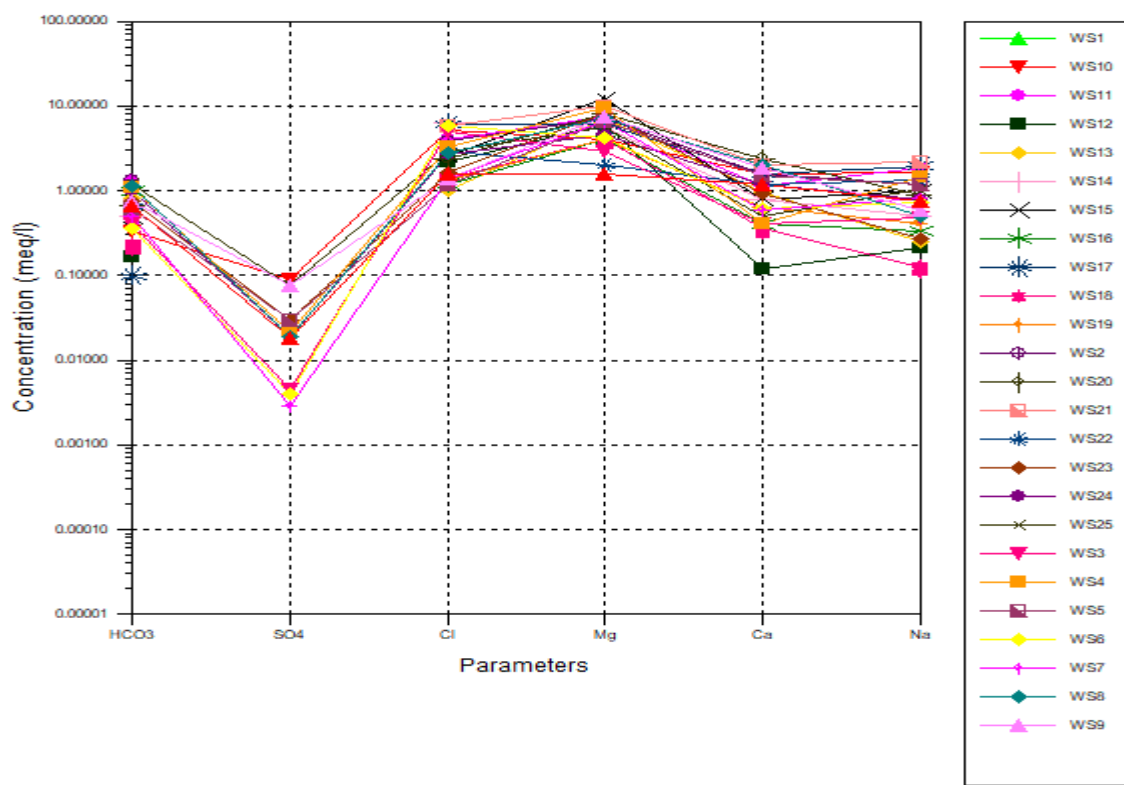
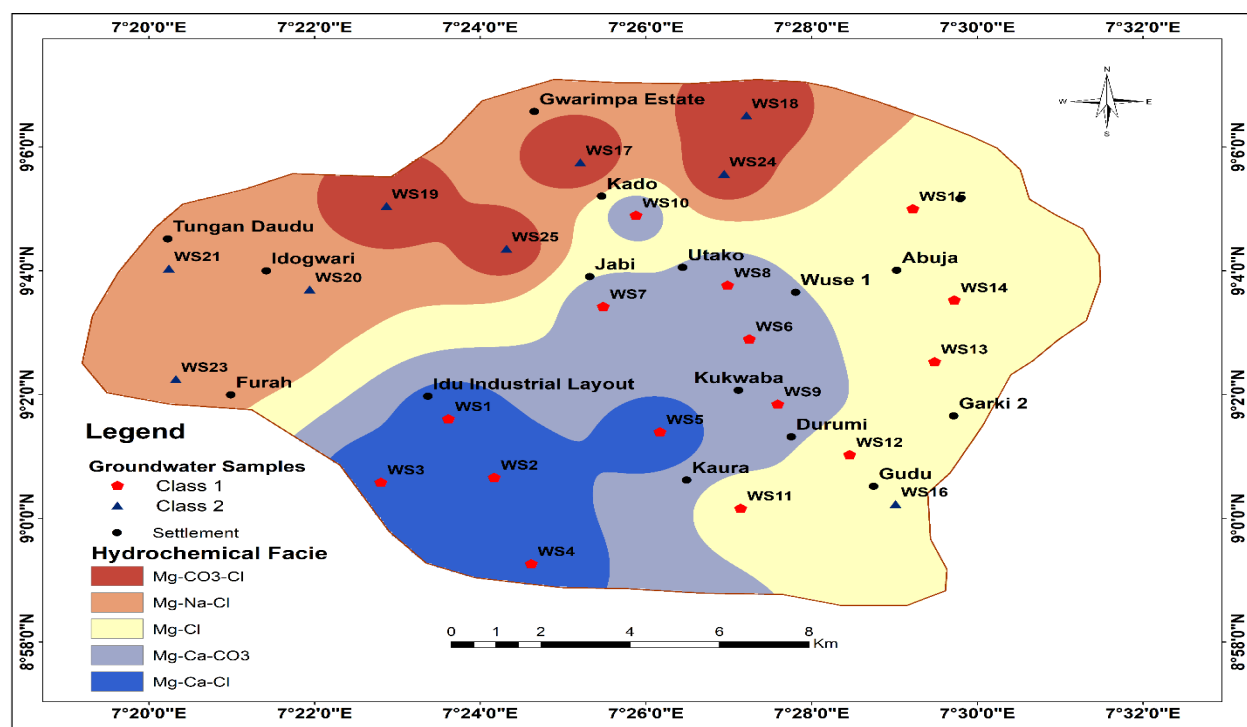**Fig. 3** Schoeller Diagram Displaying the Concentration of Cations and Anions

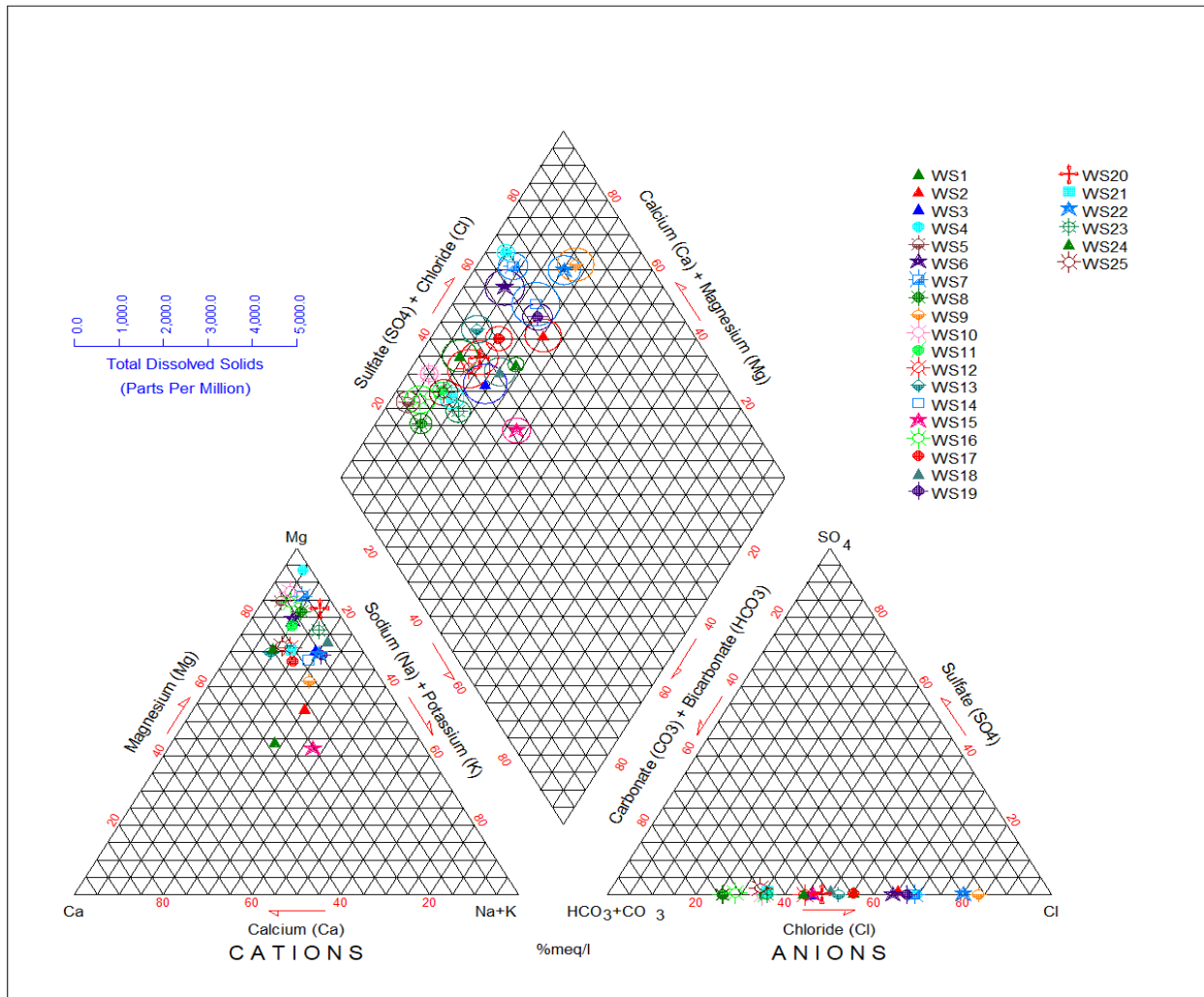**Fig. 4.** Spatial Dispensation Map showing the Water Type of the Area

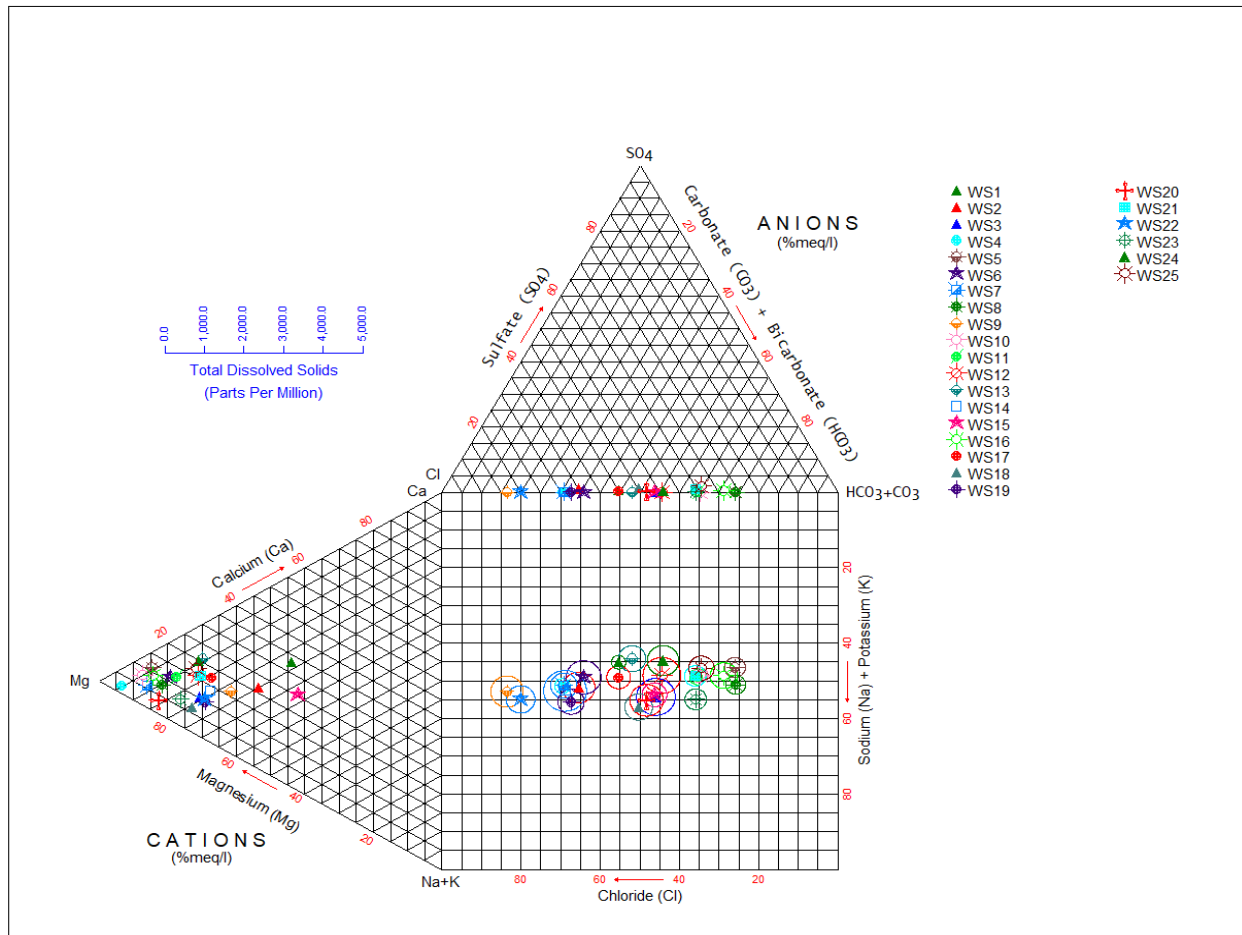**Fig. 5** Piper Diagram showing the Constituent of Groundwater in the Research Area

Fig. 6 Durov Diagram showing the Constituent of Groundwater in the Research Area

Correlation of Major Ions

In general, groundwater with pH levels ranging from a lowest of 5.5 to a high of 7.0 was considered to be relatively acidic, particularly on the southeast side (boreholes) where it was dominated by quarzitic rock formations. Generally, due to the reaction of atmospheric carbon dioxide, rainwater is mildly acidic, rendering the rainwater slightly acidic, as per (Isa et al. 2012) (Table 1):

$$H_2O + CO_2 \rightarrow H_2CO_3 \qquad (3)$$

It is possible to break down carbonate acid in water on the basis of (Hidalgo and Cruz-Sanjulian, 2001), output (HCO_3) and H^+:

$$H_2CO_3 \longleftrightarrow HCO_3^- + H^+ \qquad (4)$$
$$HCO_3 \longleftrightarrow H^+ + CO_3^{2-} \qquad (5)$$

Water alkalinity is an indicator of its neutralization capacity, which is expressed by HCO_3^-. HCO_3^- was the influential anion, which range from a lowest of 6 mg/L to a highest of 80 mg/L in the research district. The content of HCO_3^- displayed spatial heterogeneity, owing to the presence of crystalline rock in the recharge zone.

Substantial variations have been recorded in the TDS, where the TDS contents range from a lowest of 348.1 mg/l to a highest of 1092.3 mg/l. The major changes of the EC and TDS in the groundwater was based on the geochemical modifications and the human activities like utilization of fertilizer, domestic and industrial wastes in the research area. The maximum contents of TDS value portrayed an increase value of suspended ions in the groundwater samples, which intimately associated with the EC level ($r = 0.68$; $P < 0.05$), Cl^- content ($r = 0.82$; $P < 0.05$), Na^+ level ($r = 0.74$; $P < 0.05$) (Table 3). The strong association between TDS, EC, Na^+ and Cl^- demonstrated that these ions could be extracted from the same source of enrichment. In addition, there was a strong association ($r = 0.73$; $P < 0.05$) between Na^+ and Cl^-, suggesting that three sources of evaporated deposits embedded in the sediment which may have triggered groundwater acidity in the research district. From the results of the main ions, it was found that Mg^{2+} and Ca^{2+} were the prevalent cations. The level of Mg^{2+} ranges from the lowest value of 19.5 mg/l to a highest value of 145.9 mg/l. The content of Ca^{2+} fluctuates between 2.4 to 48.1 mg/l.
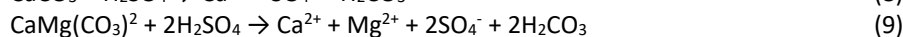
Calcite and dolomite precipitation or silicate rock dissolution may have induced high calcium and magnesium concentrations. The potential sources of hardness, typical in the granite regions, are Mg^{2+} and Ca^{2+}. There was a clear association between groundwater hardness and Mg^{2+} (r = 0.746) and Ca^{2+} (r = 1.00), which indicated that they came from the same origins. In the groundwater samples, the amount of potassium varied from 3.3 to 23.7 mg/L on the research district. Although high levels of potassium were deduced from human activities, like phosphate fertilizer feldspar in farmlands, most of which was noticed in the area around Jabi, weak associations between K^+ and several other key ions indicated that potassium was mainly sourced from k-feldspar or k-containing rocks (Table 3).

Table 3: Correlation Matrix of the Physico-chemical Parameters of Groundwater Samples Gathered from the Research Area

|	Temp.	pH	EC	TDS	CaCO₃	Ca²⁺	Mg²⁺	Na⁺	K⁺	Fe³⁺	Cl⁻	NO₃⁻	SO₄²⁻	HCO₃⁻	CO₃²⁻
Temp.	1.00														
Ph	0.05	1.00													
EC	-0.06	-0.64	1.00												
TDS	-0.25	0.37	0.68	1.00											
CaCO₃	-0.39	-0.13	0.24	0.16	1.00										
Ca²⁺	-0.08	-0.39	0.75	-0.09	0.29	1.00									
Mg²⁺	0.39	-0.28	0.47	-0.35	-0.32	0.77	1.00								
Na⁺	-0.16	-0.56	0.92	0.74	0.30	0.69	0.29	1.00							
K⁺	-0.05	-0.22	0.67	-0.45	0.02	0.54	0.39	0.66	1.00						
Fe³⁺	0.05	-0.26	0.45	-0.06	-0.21	0.15	0.27	0.28	0.08	1.00					
Cl⁻	0.01	-0.62	0.83	0.82	0.22	0.48	0.25	0.73	0.25	0.62	1.00				
NO₃⁻	-0.15	-0.37	0.50	-0.27	0.32	0.17	0.19	0.57	-0.06	-0.26	0.39	1.00			
SO₄²⁻	1.00	-1.00	1.00	-1.00	1.00	1.00	1.00	1.00	1.00	1.00	1.00	1.00	1.00		
HCO₃⁻	0.22	0.14	0.15	0.01	-0.18	0.19	0.15	0.14	0.07	0.04	-0.12	-0.20	-1.00	1.00	
CO₃²⁻	0.29	0.03	0.16	0.08	-0.09	0.07	-0.12	0.14	0.10	0.26	0.24	-0.26	1.00	0.61	1.00

Ionic Ratio

The prevalent cations and anions in the research area are magnesium, calcium, bicarbonate and chloride. The occurrence of basement rocks in the research area probably linked to the occurrence of Ca^{2+} and Mg^{2+} in the groundwater, although the precipitation of silicates may lead to Ca^{2+} and Mg^{2+} in the groundwater. The breakdown of calcite and dolomite can be seen by the Ca^{2+}/Mg^{2+} ratio of the groundwater. A molar ratio of Ca^{2+}/Mg^{2+} equal to one implies breakdown of dolomite minerals, whereas a higher ratio may reflect a substantial input from the rocks to calcite. The breakdown of silicate minerals into the groundwater may reflect a Ca^{2+}/Mg^{2+} ratio higher than 2. Although 64% of the groundwater samples posses a Ca^{2+}/Mg^{2+} ratio between 1 and 2, 30% of the samples own a ratio > 2 in calcite breakdown, which revealed the influence of silicate rocks that add magnesium and calcium to groundwater. Just a little sample (roughly 6%) were reflective of dolomite disposition with a ratio of Ca^{2+}/Mg^{2+} < 1 (Fig. 7a). The ratio of Ca^{2+}/Mg^{2+} change from the south to the northeastern and southwestern regions of the research area (Fig. 8a). Owing to increase in magnesium content related to the weathering of silicate and carbonate rocks in the recharge region, the ratio was the greatest in the Idu Industrial Layout on the southwestern side. In the central and western segments of the research district, the ratio declined with the distance from the weathering regions to the discharge regions (Fig. 8a). The following reactions ((6) to (9)) in natural processes could describe the dissolution of carbonate minerals (Kura et al. 2013):

$$CaCO_3^- + H_2CO_3^- \rightarrow Ca^{2+} + 2HCO_3^- \tag{6}$$
$$CaMg(CO_3)^2 + H_2CO_3 \rightarrow Ca^{2+} + Mg^{2+} + 4HCO_3^- \tag{7}$$
$$CaCO_3 + H_2SO_4 \rightarrow Ca^{2+} + SO_4^- + H_2CO_3 \tag{8}$$
$$CaMg(CO_3)^2 + 2H_2SO_4 \rightarrow Ca^{2+} + Mg^{2+} + 2SO_4^- + 2H_2CO_3 \tag{9}$$

In carbonate rocks, precipitation is a simple and natural weathering reaction (Drever, 1988). In groundwater, the 1:2 ratios of Ca^{2+}/HCO_3^- and 1:1 equal ratio of $Ca^{2+} + Mg^{2+}/HCO_3^-$ is described. The average scores of the Ca^{2+}/HCO_3^- ratio was 0.82, which was similar to the ratio of 1:2 and reflected the importance effect of dissolution in the host rocks. The average ratio of $Ca^{2+} + Mg^{2+}/HCO_3^-$ in groundwater was 2.06, which is also close to the equivalence ratio of 1:1, which means that about 71% of the HCO_3^- is connected to Ca^{2+} and Mg^{2+}. The less content of $Ca^{2+} + Mg^{2+}/HCO_3^-$ was found in roughly 7% of the samples that suggestive of several origins of HCO_3^- like silicate weathering in the host rock. About 22% of the samples displayed a higher ratio of $Ca^{2+} + Mg^{2+}$ to HCO_3^-, which indicates that Cl^- and SO_4^{2-} balanced the abundance of Ca^{2+} and Mg^{2+}. Since Ca^{2+}, Mg^{2+}, SO_4^{2-} and HCO_3^- are derivation of calcite, dolomite, and gypsum dissolution, the diagram of $Ca^{2+}+Mg^{2+}$ against $HCO_3^-+SO_4^{2-}$ will be similar to 1:1 side. If the dominant mechanism is ion exchange, due to abundance $SO_4^{2-} + HCO_3^-$, the parameters begin to move to the right. It is possible to describe the ion exchange reaction as follows:

$$0.5Ca^{2+}\text{-}Clay_2 + Na^+ \rightarrow 0.5Ca^{2+} + Na^+\text{-}Clay \tag{10}$$
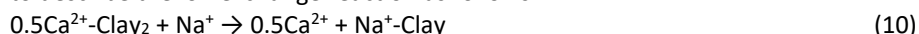
If the sites prevail over the intermediate line, the effective reaction for surplus $Ca^{2+} + Mg^{2+}$ over $SO_4^{2-} + HCO_3^-$ was the reverse ion exchange, which can be defined by the following reaction.

$$Na^+\text{-}Clay + 0.5Ca^{2+} \rightarrow Na^+ + 0.5Ca^{2+}\text{-}Clay_2 \tag{11}$$
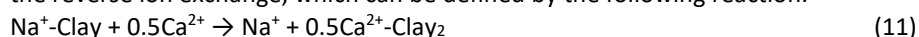
The mean ratio of $Ca^{2+} + Mg^{2+}/HCO_3^- + SO_4^{2-}$ was 0.98. As displayed in the plot, majority (69.1%) of the samples were scattered near to the 1:1 axis, suggesting that the dissolution of calcite in the host rock may result in the presence of Ca^{2+} and Mg^{2+} in the groundwater.

Additionally, about 10.9% of the samples dropped over the intermediate line, suggesting that the reverse ion exchange appeared to be the prevalent ion exchange reaction accountable for the greater ratio of HCO_3^- and SO_4^{2-} in the groundwater (Fig. 7b).

The $Ca^{2+} + Mg^{2+}$ against Cl^- and Na^+/Cl^- against Cl^- diagram certainly showed that the salinity inflated with a decline in Na^+/Cl^- and a rise in $Ca^{2+} + Mg^{2+}$, which could be as a result of reverse ion exchange in the clay/weathered strata (Fig. 7c, 7d).

The aquifer pattern perhaps oxidizes soluble Na^+ in return for tied Ca^{2+} and Mg^{2+}. On the western and northern side of the area, Na^+ was a prevalent cation and Cl^- was a dominated anion, primarily belong to the second group of clusters. The high Na^+ and Cl^- content in the groundwater may be attributed to the weathering of silicate rocks, the mechanism of evapotranspiration, and/or the infiltration of water that is enriched in soil CO_2.

Owing to the seawater mingling with the groundwater, the Cl^-/HCO_3^- ratio will display the effect of salinization. Cl^-/HCO_3^- to Cl^- ratios varied between 0.13 to 4.10 and displayed a good high linear relationship with the level of Cl^- (r = 0.79, P < 0.01) (Fig. 7e). Roughly 90% of groundwater samples displayed Cl^-/HCO_3^- ratios lesser than 0.5, which indicates that the groundwater was natural or freshwater

Other samples were between the 0.5 - 7.1 Cl^-/HCO_3^- ratios, which indicated that salinization influenced the water marginally or significantly. The spatial dispensation map of Cl^-/HCO_3^- ratio showed that the natural water mainly dominated the eastern segment of the study area. Nevertheless, salinization affected the groundwater in the western and northern segments of the research district, which was thought to be influenced by saline water (Fig. 8b).

The correlation between Na^+ - Cl^- has often utilized to describe the mechanism that regulates the salinity in many parts of the world (Dixon and Chiswell, 1992). The source of sodium values can come from various mechanisms in the groundwater. The mean ratio of Na^+/Cl^- was 2.80 in the research district, which showed a greater Na^+ levels over the Cl^- (Fig. 7f). Most of the samples displayed a Na^+/Cl^- ratio equivalent to or above 1 that perhaps reflect sodium, which was obtained from the silicate weathering. The reaction of the hornblende minerals to the carbonate acid in the water defined by bicarbonate as a one of the prevalent anions in the groundwater is silicate weathering, equivalent to the region studied (Fig. 3).

In the groundwater, halite is a major derivation of Na^+ and Cl^-; due to the cation exchange, the ratio differs spatially (Falcone et al., 2008). In many countries especially the arid and semiarid countries with less yearly rainfall of below < 700 mm, the accessibility of clear halite for breakdown in the soil profile might rise. The ratio of Na^+/Cl^- equivalent to 1 suggested that the level of sodium in the water samples may be accountable for halite breakdown. As per the spatial dispensation map of the Na^+/Cl^- ratio, most of the research district was occupied with a ratio above 1.5, which showed the function of silicate weathering as the origin of Na^+ in the research district (Fig. 8c). Areas near Idogwari, Tungan Dudu and Furah on the eastern side reflect a ratio of close to one. The salinity of groundwater can also

influence the development of salt strata by seeping from the top soil via evaporation in a tropical environment. The Na^+/Cl^- decreased significantly with increasing EC in the Na^+/Cl^- vs EC map, together with a greater Na^+/Cl^- ratio in boreholes samples (Class 1), suggesting that the Na^+ derived from the phase of silicate weathering (Fig. 7d).

In addition, majority of the samples were plotted parallel to the electrical conductivity direction (Fig. 7d) thereby suggesting the impact of evaporation to elevated sodium content.

From the east and southwestern to a small area in the northwestern side of the research district, the electrical conductivity increased steadily (Fig. 8d). The presumed district for the evaporation process, most of which were found in the boreholes (Class 1), displayed higher values of electrical conductivity. Around the eastern edge of the research district, the silicate weathering mechanism was discovered, which was guided by the borehole samples (Fig. 8d). (Fig. 8d).
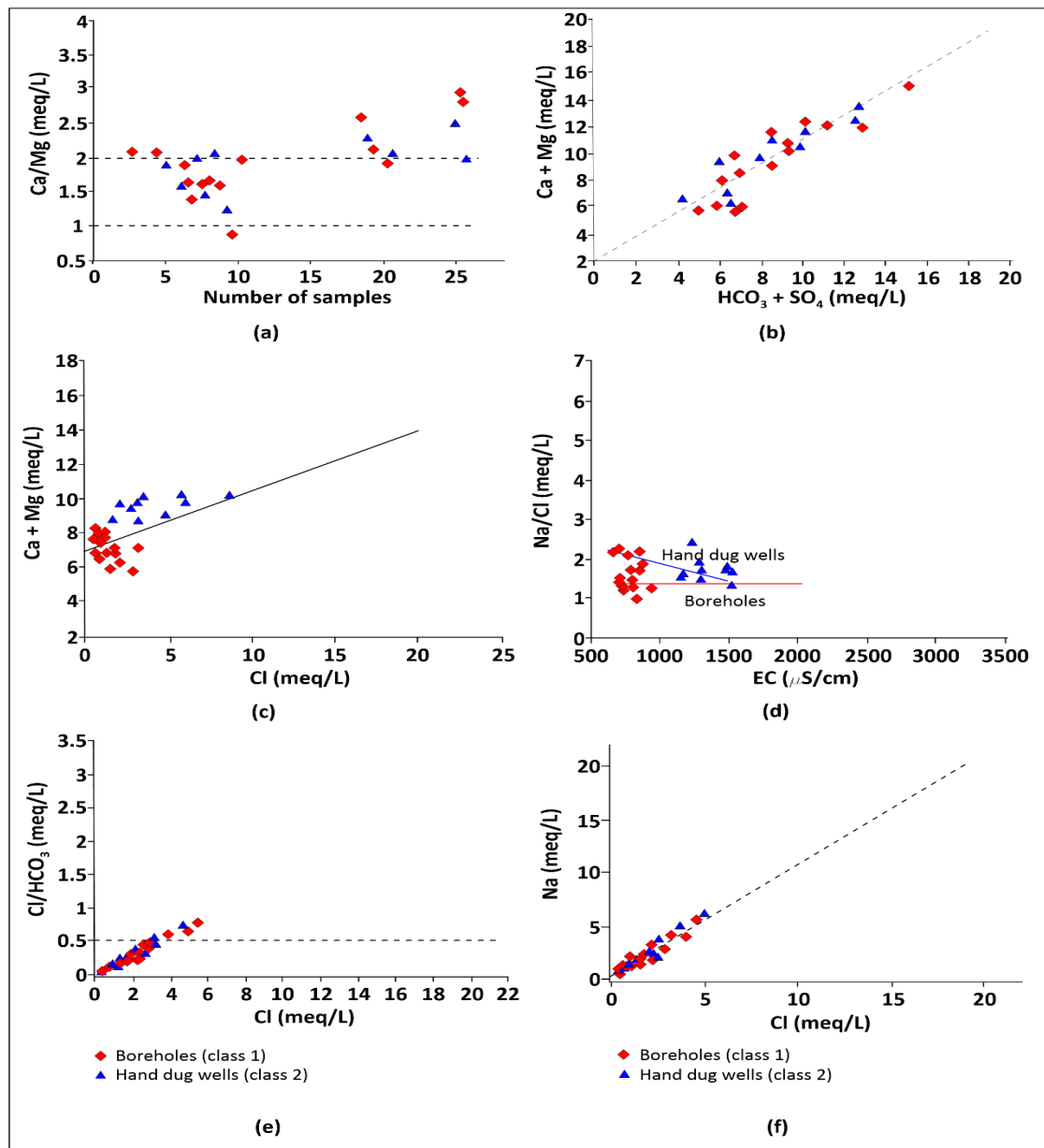

Fig. 7 Distribution of Ionic Ratios for Major Groundwater Ions from the Study Area
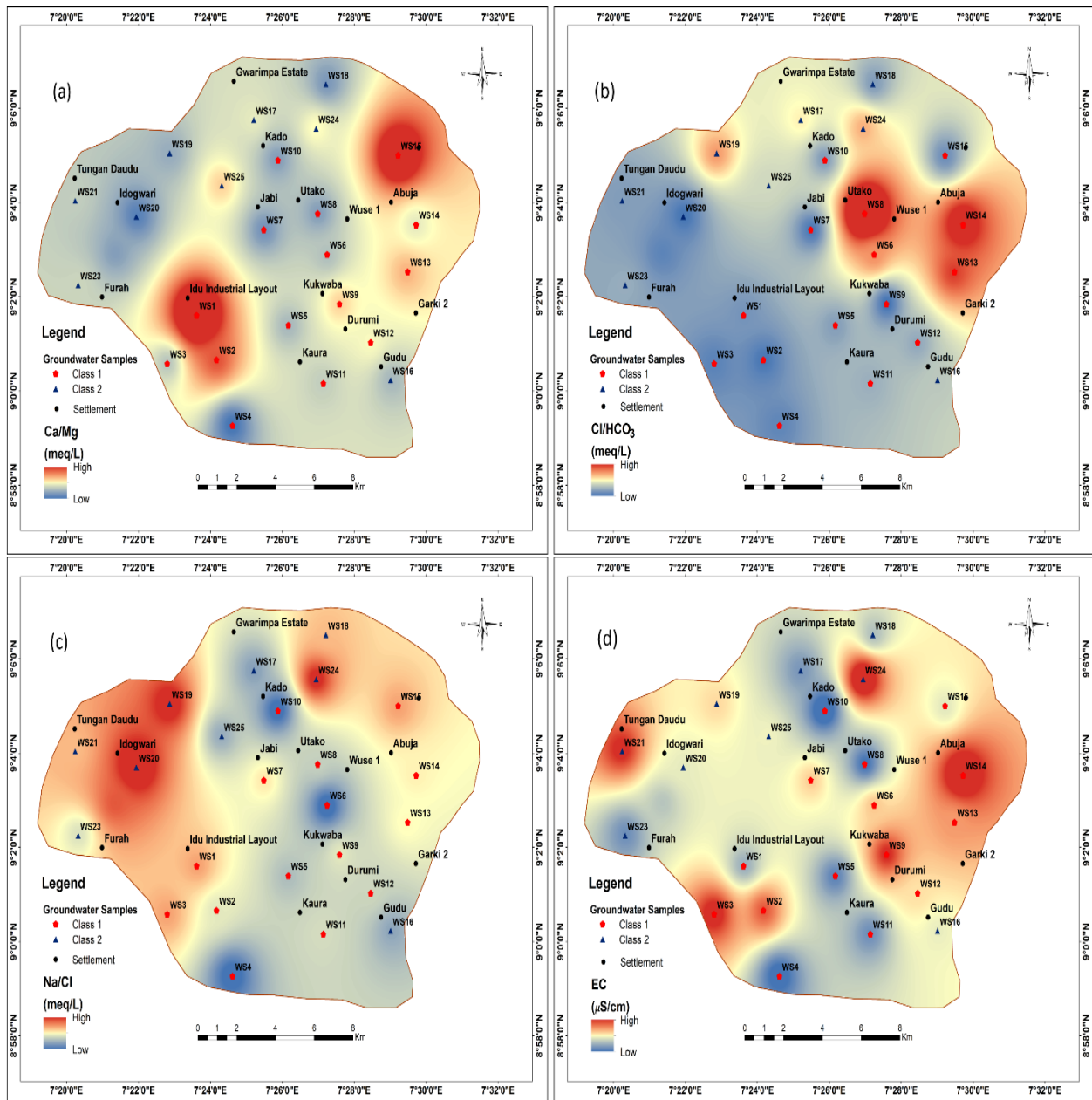
Fig. 8 Spatial Dispensation Map of (a) Ca/Mg ratio, (b) Cl/HCO3 ratio, (c) Na/Cl ratio, and (d) Electrical Conductivity, of Groundwater in Idu and Environs

Gibbs's diagram

Numerous aspects govern groundwater chemistry, which can be linked to the natural state of the aquifer, mineralogy of the underlying lithology and weather conditions. In order to explain the natural system that governs groundwater chemistry, like rainfall hegemony, rock weathering hegemony, and evaporation and activity hegemony, Gibbs (1970) recommended TDS against $Na^+/(Na^+ + Ca^{2+})$ for positive ions and TDS against $Cl^-/(Cl^-+HCO_3^-)$ for negative ions. The whole samples mapped fall into category one on the basis of the Gibbs diagram, and 97% of category two samples could have been affected by rock weathering activity (Fig. 9). Just 3% of the entire samples plotted on the evaporation-precipitation dominance area (Class 1) and (Class 2) (Fig. 9). It appears that on the eastern edge of the research district, the ion chemistry of fresh groundwater (Class 1) generally relates to the carbonate and silicate weathering process. Nevertheless, evaporation was the major constituent that largely regulate the groundwater chemistry in the north and western portions where the hand dug wells (Class 2) sampling wells were established.
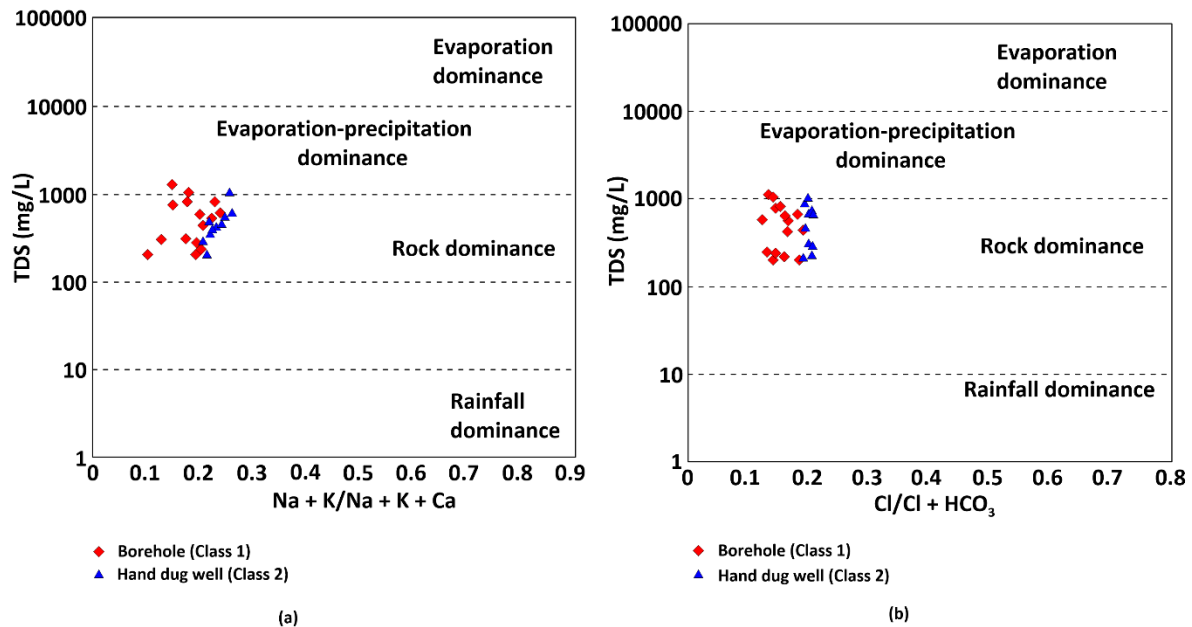
Fig. 9 Gibbs Diagrams Interpreting Groundwater Constituent of the Area.

Saturation Index

The geochemistry of the groundwater is controlled by the interplay between the groundwater and the host rocks. The estimation of mineral equilibrium can foresee the thermodynamic influence over the groundwater formulation that has been balanced with different minerals (Deutsch, 1997). The saturation index was used to anticipate the affective subsurface mineralogy from groundwater dataset, without obtaining solid state samples and analyzing the mineralogy (Deutsch, 1997). The saturation index (SI) for groundwater samples were determined adopting computer geochemical software PHREEQC, which can be characterized as

$$SI = \log \left(\frac{IAP}{K} \right) \tag{12}$$

where IAP stand for ion activity product and K stand for equilibrium constant. When equilibrium showed SI = 0; the groundwater is supersaturated when SI > 0, it indicated that rainfall is required to obtain steady-state. When SI < 0, the groundwater is under saturated; which showed that dissolution is needed to attain equilibrium. The first category displayed mildly separate action from hand dug wells (Class 2) with respect to its carbonate minerals (Table 4). In the borehole samples (Class 1), groundwater was supersaturated in contrast to the calcite and under saturated in comparison with the dolomite and aragonite. In the hand dug well samples (Class 2), groundwater was supersaturated with calcite, dolomite, and aragonite. The super saturation of groundwater with these carbonate minerals indicated that these carbonate minerals were the primary factors in the host rock. Moreover, the lesser saturation of these minerals has affected the chemical constituents of the groundwater. The evaporated minerals like, halite, gypsum, and anhydrite were under saturated in the whole groups, suggesting that the dissolved constituent of Na^+, Cl^-, Ca^{2+}, and SO_4^{2-} content was not restricted by mineral steady-state.

Table 4: Statistical Results of Saturation Indicators of Minerals Constituent of Groundwater Utilizing PHREEQC.

	Anhydrite	Aragonite	Calcite	Dolomite	Gypsum	Halite
Class 1						
Min	-3.125	-0.354	-0.163	-2.118	-3.241	-6.527
Max	-0.412	0.394	0.571	0.322	-1.110	-4.918
Mean	-1.871	-0.065	0.064	-0.079	-1.432	-5.261
CV	0.184	0.021	0.018	0.093	0.182	0.162
SD	0.376	0.214	0.109	0.254	0.364	0.384
Class 2						
Min	-3.011	-0.201	-0.145	-0.638	-2.848	-6.189
Max	-0.356	0.312	0.380	0.467	-0.882	-4.344
Mean	-1.287	0.066	0.078	0.182	-1.242	-5.182
CV	0.217	0.029	0.030	0.104	0.366	0.158
SD	0.321	0.136	0.124	0.208	0.570	0.340

Conclusions

In order to examine spatial aspects and systems regulating the chemical properties of groundwater in Idu and environs, a combination of statistical methods and geochemical processes has been applied. The Mg-Cl type, which covers major portions of the eastern segment of the research district, and changes in the Mg-CO$_3$-Cl and Mg-Na-Cl types on the north and western parts and Mg-Ca-CO$_3$ and Mg-Ca-Cl types on the central and southern segments of the research district, were generally the prevalent hydrogeochemical facies of groundwater. The chemistry of the groundwater was basically influenced by rocks weathering. The main hydrogeochemical pathways influencing the groundwater hardness in the study area was water/rock contacts, like carbonate mineralization and silicate weathering. The high magnesium value observed may be credited to the disintegration of carbonate rocks on the eastern segments of the area, while evaporation was the prevalent mechanism in regard to the chloride on the northern and western districts of the research district. According to the hierarchical cluster examination of sampling wells, the freshwater type is represented by samples of the first group apportioned on the east, south, and central regions. The Gibbs diagram revealed that the hydrochemistry of these classes was primarily affected by rock domination, such as the weathering of carbonate and silicate rocks. The groundwater type in Class 2 slowly transformed to salt water around the north-western part of the area. The Gibbs plot definitely demonstrates the function of the host rock mechanisms in the groundwater chemistry of the area. In the entire two classes, groundwater samples were saturated with respect to calcite and sub-saturated with regard to gypsum minerals. Careful monitoring could be recommended for the salinity control in the locations with salty water, which were defined by spatial dispensation maps in the ArcGIS software.

References

APHA. (2005), Standard methods for the examination of water and wastewater. *American Public Health Association, American Water Works Association, Water Environment federation, Washigton, DC, USA*.

Appelo, G.A.J., Postma, D., (1994). Geochemistry, groundwater and pollution. *A.A. Balkema,Rotterdam*, pp 536

Aris, A.Z., Praveena, S.M., Abdullah, M.H., (2010). The influence of seawater on the chemical composition of groundwater in a small island: case study of Mankun Island. *East Malaysia. J. Coa. Res*, 28(1), 181-194

Demirel, Z., Turkmen, S., (2001). The hydrogeological investigation of Kazanlı region. *Soda Factory AG, Kazanlı-Mersin, unpublished report*.

Deutsch, W.J., (1997). Groundwater Geochemistry: Fundamentals and Application to Contamination, CRC, BocaRaton, Fla, USA.

Dixon, W., Chiswell, B. (1992). The use of hydrochemical sections to identify recharge areas and saline intrusions in alluvial aquifers, southeast Queensland, Australia. *J. Hydrolo*, 35(1-4), 259-274

Drever, J.I., (1988). The Geochemistry of Natural Waters, vol. 2, Prentice Hall, New Jersey, NJ, USA.

Falcone, A.R., Falgiani, A., Parisse, B., Petitta, M., Spizzico, M., Tallini, M., 2008. Chemical and isotopic (δ^{18}O‰, δ^{2}H‰, δ^{13}C‰, ^{222}Rn) multi tracing for groundwater conceptual model of carbonate aquifer (Gran Sasso INFN underground laboratory-central Italy). *J. Hydrolo*, 357(3-4), 68-388.

Gibbs, R.J., (1970). Mechanism controlling world water chemistry. *Sci*. 170, 1088-109.

Hamzah, Z., Aris, A.Z., Ramli, M.F., Juahir, H., Narany, T.S., (2017). Groundwater quality assessment using integrated geochemical methods, multivariate statistical analysis, and geostatistical technique in shallow coastal aquifer of Terengganu, Malaysia. Arab. *J. Geosci*, 10, 49.

Hanshaw, B.B., Back, W., (1979). Major geochemical processes in the evolution of carbonate-aquifer systems. *J. Hydrolo*. 43 (1-4), 287-312.

Hidalgo, M.C, Cruz-Sanjulian, J., (2001). Groundwater composition, hydrochemical evolution and mass transfer in a regional detrital aquifer (Baza basin, southern Spain). *Applied. Geochem*, 16, 745-758.

Ifediegwu, S.I., (2019). Groundwater recharge estimation using chloride mass balance: a case study of Nsukka local government area of Enugu State, Southeastern, Nigeria. *Model. Earth Syst. Environ*.

Ifediegwu, S.I., Onyeabor, F.C., Nnamani, M.C., (2019). Geochemical evaluation of carbonate aquifers in Ngbo and environs, Ebonyi State, southeastern, Nigeria. *Model. Earth Syst. Environ*.

Isa, N.M., Aris, A.Z., Sulaiman, W.N.A.W., (2012). Extent and severity of groundwater contamination based on hydrochemistry mechanism of sandy tropical coastal aquifer. *Sci. Total Environ*, 438, 414-425

Jalali, M. (2005). Major ion chemistry in the Bahar area, Hamadan, western Iran. *Environ. Geol*, 47, 763-772.

Journel, A., Keith, L.H., (1988). Non-parametric geostatistics for risk and additional sampling assessment in Principles of Environmental Sampling. *American Chemical Society, Washington, DC, USA*.

Narany, T.S., Ramli, M.F., Aris, A.Z., Sulaiman, W.N.A., Juahir, H., Fakharian, K., (2014). Identification of the hydrogeochemical processes in groundwater using classic integrated geochemical methods and geostatistical techniques, in Amol-Babol Plain, Iran. *Hindawi Publishing Corporation Sci World J*.

Nas, B., Berktay, A., (2010). Groundwater quality mapping in urban groundwater using GIS. *Environ. Monit. Assess*, 160(1-4), 215-227.

Ohwoghere-Asuma, O., Essi, O.E., (2017). Investigation of Seawater Intrusion into Coastal Groundwater Aquifers of Escravos, Western Niger Delta, Nigeria. *J. Appl. Sci. Environ. Manage*, 21(2), 362-369.

Ravikumar, P., Somashekar, R.K., Prakash, K.L., (2015). A comparative study on usage of Durov and Piper diagrams to interpret hydrochemical processes in groundwater from SRLIS river basin, Karnataka, India. *Elixir. Earth Sci*, 80, 31073-31077.

Reddy, A.G.S., Kumar, K.N., (2010). Identification of the hydrogeochemical processes in groundwater using major ion chemistry: a case study of Penna-Chitravathi river basins in southern India. *Environ. Monit. Assess*, 170, 365-382.

Retnam, A., Zakaria, M.P., Juahir, H., Aris, A.Z., Zali, M.A., Kasim, M.F., (2013). Chemometric techniques in distribution characterisation and sourceapportionment of polycyclic aromatic hydrocarbons (PAHS) inaquaculture sediments in Malaysia. *Mar. Pollut. Bull*, 69, 55-66.

Salama, R.B., Otto, C.J., Fitzpatrick, R.W., (1999). Contributions of groundwater conditions to soil and water salinization. *Hydrogeo. J*, 7(1), 46-64.

Sisodia, R., Moundiotiya, C., (2006). Assessment of the water quality index of wetland Kalakho lake, Rajasthan, India. *J. Environ. Hydrol*, 14, 1-11.

Triki, I., Trabelsi, N., Zairi, M., Dhia, H.B., (2013). Multivariate statistical and geostatistical techniques for assessing groundwater salinization in Sfax, a coastal region of eastern Tunisia. *Desalin. Water Treat*. 1-10.